The embedding method for electromagnetics

1998 J. Phys. A: Math. Gen. 31 8495

(http://iopscience.iop.org/0305-4470/31/42/009)

J. Phys. A: Math. Gen. **31** (1998) 8495–8510. Printed in the UK PII: S0305-4470(98)92909-2

The embedding method for electromagnetics

J E Inglesfield

Department of Physics and Astronomy, University of Wales Cardiff, PO Box 913, Cardiff CF2 3YB, UK

Received 30 March 1998

Abstract. A new method is derived for solving Maxwell's equations for a region of space, region I, joined onto region II, which may be a finite dielectric or an extended substrate. This is based on a variational principle in which a trial field is defined explicitly only in region I, the solution of Maxwell's equations in region II being included through an embedding operator defined on the boundary of region I with II. This operator is the inverse of a non-local boundary impedance. The method is applied to calculating the normal modes of an array of dielectric slabs, semi-infinite dielectrics separated by vacuum, and modes confined in a three-dimensional box with conducting walls. Plane wave basis functions are used to expand the electric field in region I, and the method shows excellent convergence in all cases. Approximate solutions of Laplace's equation can occur, corrupting the solutions of Maxwell's equations with finite frequency. It is shown how these can be suppressed.

1. Introduction

This paper describes a new method for solving Maxwell's equations for the propagation of electromagnetic waves in dielectric structures. There is currently much theoretical [1–5] and experimental [1, 6–9] interest in different photonic structures—two- and three-dimensional arrays of dielectrics [6, 8], arrays with defects [10] and so on—because of the possibility of novel propagation effects [1]. The classical techniques of explicitly matching electric and magnetic fields across a dielectric interface[11] become very involved for such geometries, and other methods for finding the electromagnetic modes have been developed. Plane wave basis set expansions of the field are widely used for finding photonic bandstructures in periodic arrays of dielectrics [2–4, 12, 13], and spatial discretization methods have been developed [14, 15] which can be used in a wide range of geometries [16]. Green function scattering methods, analogous to the KKR method for electronic band structures, have also been applied to photonics [17–19].

The embedding method which we shall describe in this paper was originally developed for solving the electronic Schrödinger equation in a region of space (region I) joined onto some substrate (region II) [20]. The idea of embedding is that the Schrödinger equation may be solved explicitly only in region I, the effect of the substrate being included by adding an embedding potential on to the Hamiltonian for region I. This embedding potential ensures that the solutions of the Schrödinger equation in region I have the right amplitude and derivative to match on to the solutions in region II. The method has been used to include the effects of the semi-infinite substrate in surface calculations [21], the embedding potential (complex in this case) broadening the discrete states in the finite surface region into continuum states. It has also proved useful in solving the Schrödinger equation for electrons

0305-4470/98/428495+16$19.50

confined in a region of space, which may have complicated geometry, by an infinite potential barrier [22]. Here the embedding potential provides the right reflection boundary conditions, and it permits a basis set expansion of the wavefunction in the confined region. Region II need not be an extended substrate: the embedding potential can replace the potential in an enclosed region, for example replacing the deep potential inside the atomic core [23].

In this paper we shall apply the embedding method to solving Maxwell's equations, and we envisage analogous applications to the Schrödinger equation case. A variational expression is derived which only contains a trial electric field in region I, which we want to treat explicitly. The rest of space, region II, which might be an enclosed dielectric or a substrate, is replaced by an embedding operator defined on the boundary between regions I and II. The frequency-dependence of the embedding operator has to be built into the variational expression, and this is connected with the normalization of the fields in region II. In region I, we can then solve Maxwell's equation in any way we choose, for example using a basis set expansion, and the embedding operator ensures that the parallel components of the electric and magnetic fields match across the boundary with region II.

Variational principles form the basis of many methods of solving Maxwell's equations [24], and using them in a restricted region of space is also well known [25–28]. The rest of the system can be replaced by electric and magnetic sources on the boundary [29, 30], and Green function techniques have been used to handle an external region in finite element methods [27, 31, 32]. These ideas are closely related to the ideas in this paper, though the derivation, form, and method of applying the embedding variational principle are new, to the best of our knowledge. The embedding operator, which gives the parallel component of the magnetic field at the boundary of region II in terms of the electric field, is the inverse of a non-local form of the boundary impedance [33]. This concept is also widely used in solving electromagnetic problems [34].

The plan of this paper is as follows. In section 2 we shall set up the embedding variational principle for solutions to Maxwell's equations in region I joined onto region II, defining the trial wavefield explicitly only in region I, with region II replaced by the embedding operator on the boundary. In section 3 we shall consider the generalized matrix eigenvalue equation obtained with a basis set expansion of the electric field. In section 4 the band structure of waves travelling normal to a one-dimensional array of dielectric slabs is calculated, and excellent convergence is achieved; because the plane waves are used to expand the field only *between* the slabs, much better convergence is obtained than with a plane wave expansion through the whole of space (this is one of the advantages of the embedding method). In the application described in section 5, to waves propagating between dielectric slabs with dielectric constant less than 1 (so that total internal reflection can occur), an important problem shows up. When the electric field has a component normal to the boundary of region I, Laplace solutions can occur; with a finite basis set expansion, these may have finite frequency in the variational expression, thereby corrupting the solutions of Maxwell's equations in which we are interested. Fortunately we have resolved this problem, and this is explained in section 5. Finally, in section 6 we apply the method to electromagnetic waves confined by conducting walls, calculating the spectral density of the discrete modes broadened by the lossy surrounding medium.

2. Embedding variational principle

From Maxwell's equations, electromagnetic modes with frequency ω satisfy the eigenvalue equation

$$\nabla \times \nabla \times \boldsymbol{E} = \epsilon(\boldsymbol{r})\frac{\omega^2}{c^2}\boldsymbol{E} \tag{1}$$

where $\epsilon(\boldsymbol{r})$ is the spatially-varying dielectric constant, and we shall assume that $\mu = 1$ everywhere. The eigenvalue $k^2 = \omega^2/c^2$ is then given by stationary values of

$$k^2 = \frac{\int \mathrm{d}\boldsymbol{r}\, \boldsymbol{E} \cdot (\nabla \times \nabla \times \boldsymbol{E})}{\int \mathrm{d}\boldsymbol{r}\, \epsilon \boldsymbol{E} \cdot \boldsymbol{E}} \tag{2}$$

with respect to variations in $\boldsymbol{E}(\boldsymbol{r})$ (which we shall assume to be real) [24]; the integrals are over all space, and we assume that $\boldsymbol{E}$ vanishes at large $\boldsymbol{r}$. Using the vector identity that

$$\nabla \cdot (\boldsymbol{F} \times \nabla \times \boldsymbol{E}) = (\nabla \times \boldsymbol{F}) \cdot (\nabla \times \boldsymbol{E}) - \boldsymbol{F} \cdot (\nabla \times \nabla \times \boldsymbol{E}) \tag{3}$$

and the divergence theorem to transform the div term into a vanishing surface integral, this can be written as [24]

$$k^2 = \frac{\int \mathrm{d}\boldsymbol{r}\, (\nabla \times \boldsymbol{E}) \cdot (\nabla \times \boldsymbol{E})}{\int \mathrm{d}\boldsymbol{r}\, \epsilon \boldsymbol{E} \cdot \boldsymbol{E}}. \tag{4}$$

This form has the advantage that the Hermiticity of the integrand in the numerator is explicit.

Having set up the basic variational principle, we now consider the embedding problem where we have two regions I and II joined onto one another. Our aim is to obtain a variational expression for k^2 with a trial function defined *explicitly* only in region I [20]. We first split up each integral in (4) into separate integrals over I and II:

$$k^2 = \frac{\int_{\mathrm{I}} \mathrm{d}\boldsymbol{r}\, (\nabla \times \boldsymbol{E}) \cdot (\nabla \times \boldsymbol{E}) + \int_{\mathrm{II}} \mathrm{d}\boldsymbol{r}\, (\nabla \times \boldsymbol{E}) \cdot (\nabla \times \boldsymbol{E})}{\int_{\mathrm{I}} \mathrm{d}\boldsymbol{r}\, \epsilon \boldsymbol{E} \cdot \boldsymbol{E} + \int_{\mathrm{II}} \mathrm{d}\boldsymbol{r}\, \epsilon \boldsymbol{E} \cdot \boldsymbol{E}}. \tag{5}$$

Implicit in this is that there should be no surface contribution from the surface S between I and II—this requires that the surface-parallel components of $\boldsymbol{E}$ are continuous across S. Next we take an arbitrary trial function $\mathcal{E}(\boldsymbol{r})$ in region I, which we extend into region II with the exact solution $\boldsymbol{E}(\boldsymbol{r})$ of (1) at some trial value of $\omega^2/c^2 = k_0^2$. The surface-parallel components of $\boldsymbol{E}$ in II are taken to match those of $\mathcal{E}$ in I over S, and this inhomogeneous boundary condition in fact defines $\boldsymbol{E}$ uniquely in II. Using (3) and the divergence theorem (5) becomes

$$k^2 = \frac{\int_{\mathrm{I}} \mathrm{d}\boldsymbol{r}\, (\nabla \times \mathcal{E}) \cdot (\nabla \times \mathcal{E}) + k_0^2 \int_{\mathrm{II}} \mathrm{d}\boldsymbol{r}\, \epsilon \boldsymbol{E} \cdot \boldsymbol{E} - \int_S \mathrm{d}r_S\, \boldsymbol{n} \cdot (\boldsymbol{E} \times \nabla \times \boldsymbol{E})}{\int_{\mathrm{I}} \mathrm{d}\boldsymbol{r}\, \epsilon \mathcal{E} \cdot \mathcal{E} + \int_{\mathrm{II}} \mathrm{d}\boldsymbol{r}\, \epsilon \boldsymbol{E} \cdot \boldsymbol{E}} \tag{6}$$

where the third integral in the numerator is over S, and $\boldsymbol{n}$ is the normal to S, taken outwards from I into II.

The next stage is to rewrite the volume integrals through II in terms of surface integrals over S. In region II we have

$$\nabla \times \nabla \times \boldsymbol{E} = \epsilon(\boldsymbol{r}) k_0^2 \boldsymbol{E} \tag{7}$$

—k_0^2 is a parameter rather than an eigenvalue, as $\boldsymbol{E}$ satisfies the inhomogeneous boundary condition on S. Differentiating this equation with respect to k_0^2 gives

$$\nabla \times \nabla \times \frac{\partial \boldsymbol{E}}{\partial k_0^2} = \epsilon(\boldsymbol{r})\boldsymbol{E} + \epsilon(\boldsymbol{r}) k_0^2 \frac{\partial \boldsymbol{E}}{\partial k_0^2} \tag{8}$$

and multiplying (7) by $\partial \boldsymbol{E}/\partial k_0^2$ on the left, (8) by $\boldsymbol{E}$ and subtracting we obtain

$$\epsilon(\boldsymbol{r})\boldsymbol{E}\cdot\boldsymbol{E} = \boldsymbol{E}\cdot\left(\nabla\times\nabla\times\frac{\partial \boldsymbol{E}}{\partial k_0^2}\right) - \frac{\partial \boldsymbol{E}}{\partial k_0^2}\cdot(\nabla\times\nabla\times\boldsymbol{E})\,. \tag{9}$$

We now integrate through region II, substituting the vector relation (3):

$$\begin{aligned}\int_{\mathrm{II}} \mathrm{d}\boldsymbol{r}\,\epsilon\boldsymbol{E}\cdot\boldsymbol{E} &= \int_{\mathrm{II}} \mathrm{d}\boldsymbol{r}\left[\nabla\cdot\left(\frac{\partial \boldsymbol{E}}{\partial k_0^2}\times\nabla\times\boldsymbol{E}\right) - \nabla\cdot\left(\boldsymbol{E}\times\frac{\partial}{\partial k_0^2}\nabla\times\boldsymbol{E}\right)\right]\\ &= \int_S \mathrm{d}r_S\left[\boldsymbol{n}\cdot\left(\boldsymbol{E}\times\frac{\partial}{\partial k_0^2}\nabla\times\boldsymbol{E}\right) - \boldsymbol{n}\cdot\left(\frac{\partial \boldsymbol{E}}{\partial k_0^2}\times\nabla\times\boldsymbol{E}\right)\right].\end{aligned} \tag{10}$$

But $\boldsymbol{E}$ at the boundary S is fixed, so $\partial \boldsymbol{E}/\partial k_0^2 = 0$. Hence we obtain the interesting result

$$\int_{\mathrm{II}} \mathrm{d}\boldsymbol{r}\,\epsilon\boldsymbol{E}\cdot\boldsymbol{E} = \int_S \mathrm{d}r_S\boldsymbol{n}\cdot\left(\boldsymbol{E}\times\frac{\partial}{\partial k_0^2}\nabla\times\boldsymbol{E}\right). \tag{11}$$

We can now write our variational function (6) as

$$k^2 = \frac{\int_{\mathrm{I}} \mathrm{d}\boldsymbol{r}\,(\nabla\times\mathcal{E})\cdot(\nabla\times\mathcal{E}) - \int_S \mathrm{d}r_S\boldsymbol{n}\cdot[\mathcal{E}\times(\nabla\times\boldsymbol{E} - k_0^2\frac{\partial}{\partial k_0^2}\nabla\times\boldsymbol{E})]}{\int_{\mathrm{I}} \mathrm{d}\boldsymbol{r}\,\epsilon\mathcal{E}\cdot\mathcal{E} + \int_S \mathrm{d}r_S\boldsymbol{n}\cdot(\mathcal{E}\times\frac{\partial}{\partial k_0^2}\nabla\times\boldsymbol{E})} \tag{12}$$

—we have eliminated region II except for $\nabla\times\boldsymbol{E}$, the magnetic field in region II at S.

Because we are solving Maxwell's equations exactly in II, $\nabla\times\boldsymbol{E}$ can be found in terms of surface values of $\boldsymbol{E}$ by using a tensor Green function $\boldsymbol{\Gamma}$ satisfying [24]

$$\nabla_r\times\nabla_r\times\boldsymbol{\Gamma}(\boldsymbol{r},\boldsymbol{r}';k_0^2) - \epsilon(\boldsymbol{r})k_0^2\boldsymbol{\Gamma}(\boldsymbol{r},\boldsymbol{r}';k_0^2) = \mathbf{1}\delta(\boldsymbol{r}-\boldsymbol{r}'). \tag{13}$$

We adopt the same strategy as before, multiplying (7) by $\boldsymbol{\Gamma}$ and (13) by $\boldsymbol{E}$, subtracting, integrating through II, and transforming to a surface integral with the divergence theorem. This gives

$$\boldsymbol{E}(\boldsymbol{r}') = \int_S \mathrm{d}r_S\,[\boldsymbol{\Gamma}.(\boldsymbol{n}\times\nabla\times\boldsymbol{E}) + (\nabla\times\boldsymbol{\Gamma})\cdot(\boldsymbol{n}\times\boldsymbol{E})]. \tag{14}$$

If $\boldsymbol{\Gamma}$ is chosen to satisfy the homogeneous boundary on S:

$$(\boldsymbol{n}\times\boldsymbol{\Gamma}) = 0 \tag{15}$$

then $\boldsymbol{E}$ within II is given by [24]

$$\boldsymbol{E}(\boldsymbol{r}') = \int_S \mathrm{d}r_S\,(\nabla_r\times\boldsymbol{\Gamma})_{r_S,r'}\cdot(\boldsymbol{n}\times\mathcal{E}). \tag{16}$$

In particular we have

$$\nabla\times\boldsymbol{E}|_{r'_S} = \int_S \mathrm{d}r_S\,[(\nabla_r\times)(\nabla_{r'}\times)\boldsymbol{\Gamma}]_{r_S,r'_S}\cdot(\boldsymbol{n}\times\mathcal{E}) \tag{17}$$

—knowing $\mathcal{E}$ on S we can find $\nabla\times\boldsymbol{E}$ as we require. We rewrite (17) as

$$\nabla\times\boldsymbol{E}|_{r_S} = \int_S \mathrm{d}r'_S\,\boldsymbol{\Sigma}(\boldsymbol{r}_S,\boldsymbol{r}'_S)\cdot(\boldsymbol{n}\times\mathcal{E}) \tag{18}$$

where the embedding operator—a tensor—is given by

$$\boldsymbol{\Sigma}(\boldsymbol{r}_S,\boldsymbol{r}'_S) = [(\nabla_r\times)(\nabla_{r'}\times)\boldsymbol{\Gamma}]_{r_S,r'_S}. \tag{19}$$

Only the surface-parallel components of $\mathcal{E}$ appear on the right of $\boldsymbol{\Sigma}$ in (18), and only the surface-parallel components of $\nabla\times\boldsymbol{E}|_{r_S}$ are needed in (12). This means that only the surface-parallel components of the embedding operator have to be defined.

Substituting (18) into (12) gives us our embedding variational expression:

$$k^2 = \frac{\int_{\rm I} \mathrm{d}\boldsymbol{r}\, (\nabla \times \mathcal{E}) \cdot (\nabla \times \mathcal{E}) - \int_S \mathrm{d}r_S \int_S \mathrm{d}r'_S\, (\boldsymbol{n} \times \mathcal{E}) \cdot (\boldsymbol{\Sigma} - k_0^2 \frac{\partial \boldsymbol{\Sigma}}{\partial k_0^2}) \cdot (\boldsymbol{n} \times \mathcal{E})}{\int_{\rm I} \mathrm{d}\boldsymbol{r}\, \epsilon \mathcal{E} \cdot \mathcal{E} + \int_S \mathrm{d}r_S \int_S \mathrm{d}r'_S\, (\boldsymbol{n} \times \mathcal{E}) \cdot \frac{\partial \boldsymbol{\Sigma}}{\partial k_0^2} \cdot (\boldsymbol{n} \times \mathcal{E})}. \tag{20}$$

Stationary values of k^2 with respect to variations in $\mathcal{E}$ in I, and with respect to parameter k_0^2 at which the embedding operator $\boldsymbol{\Sigma}$ is evaluated, give the eigenvalues $k^2 = \omega^2/c^2$ of the system and the corresponding fields. In appendix A we shall go the other way round, proving that (20) is stationary when the field satisfies

$$\nabla \times \nabla \times \mathcal{E} = \epsilon(\boldsymbol{r}) k^2 \mathcal{E} \tag{21}$$

in I and the surface-parallel components of $\mathcal{E}$ and $\nabla \times \mathcal{E}$ match onto the solutions in II. In other words we have found the solution for I joined onto II by solving Maxwell's equations in region I only, with the extra terms involving the embedding operator $\boldsymbol{\Sigma}$ *embedding* I onto II. $\boldsymbol{\Sigma}$ is the inverse of the non-local boundary impedance [33]—this is a concept widely used in solving boundary condition problems in electromagnetism [34].

3. Applying the embedding method

The embedding variational principle can be used to find a matrix eigenvalue equation for the electric field and k^2. We expand $\mathcal{E}(\boldsymbol{r})$ in region I in terms of basis functions:

$$\mathcal{E}(\boldsymbol{r}) = \sum_i e_i \boldsymbol{F}_i(\boldsymbol{r}) \tag{22}$$

and substituting into (20) and varying with respect to the coefficients e_i we obtain the generalized eigenvalue equation

$$Ae = k^2 Be. \tag{23}$$

The matrices are given by

$$\begin{aligned} A_{ij} &= \int_{\rm I} \mathrm{d}\boldsymbol{r}\, (\nabla \times \boldsymbol{F}_i) \cdot (\nabla \times \boldsymbol{F}_j) - \int_S \mathrm{d}r_S \int_S \mathrm{d}r'_S\, (\boldsymbol{n} \times \boldsymbol{F}_i) \cdot \left(\boldsymbol{\Sigma} - k_0^2 \frac{\partial \boldsymbol{\Sigma}}{\partial k_0^2} \right) \cdot (\boldsymbol{n} \times \boldsymbol{F}_j) \\ B_{ij} &= \int_{\rm I} \mathrm{d}\boldsymbol{r}\, \epsilon \boldsymbol{F}_i \cdot \boldsymbol{F}_j + \int_S \mathrm{d}r_S \int_S \mathrm{d}r'_S\, (\boldsymbol{n} \times \boldsymbol{F}_i) \cdot \frac{\partial \boldsymbol{\Sigma}}{\partial k_0^2} \cdot (\boldsymbol{n} \times \boldsymbol{F}_j). \end{aligned} \tag{24}$$

From the structure of (24), we see that the embedding operator terms taken together appear as

$$\int_S \mathrm{d}r_S \int_S \mathrm{d}r'_S\, (\boldsymbol{n} \times \boldsymbol{F}_i) \cdot \left(\boldsymbol{\Sigma} + (k^2 - k_0^2) \frac{\partial \boldsymbol{\Sigma}}{\partial k_0^2} \right) \cdot (\boldsymbol{n} \times \boldsymbol{F}_j) \tag{25}$$

—the derivative terms provide a correction so that $\boldsymbol{\Sigma}$ is evaluated at the right value of k^2, correct to first order. Having found eigenvalue k^2 for a trial value of k_0^2, k_0^2 is set equal to this eigenvalue and the procedure iterated until the output k^2 is adequately close to the input k_0^2. In section 4 we shall show how this works in practice: the first order correction of the derivative terms not only ensures that (20) is a stationary principle, it also means that the iterative procedure converges very fast.

A problem immediately arises because (20) can take its minimum value of $k^2 = 0$ whenever $\mathcal{E}$ is a solution of Laplace's equation within region I. These solutions have zero curl in I; moreover, $\boldsymbol{\Sigma} = 0$ at $k^2 = 0$, so there is no constraint on the boundary S in this case. We would be able to avoid these solutions by taking the basis functions $\boldsymbol{F}_i$ to be transverse waves, satisfying a homogeneous boundary condition (say $[\boldsymbol{n} \times (\nabla \times \boldsymbol{F}_i)] = 0$)

over S. A solution of Laplace's equation with zero curl everywhere inside region I cannot be built up out of such functions. However, the whole idea of embedding is to tackle awkwardly shaped regions, and normally the basis functions will be transverse waves with a range of amplitude and curl over S, chosen to satisfy a homogeneous boundary condition on some simple boundary beyond S. Approximate solutions of Laplace's equation *can* be constructed out of linear combinations of these functions, even though individually they have finite curl. As these solutions are approximate, their expectation value in (20) gives finite k^2, which can lead to confusion with the fields we are really interested in—solutions of (1) with finite electric *and* magnetic fields.

Fortunately we know how many Laplace solutions can arise with any particular basis set, and their form. Every Laplace solution within I can be found from the boundary condition of specifying the normal component of $\boldsymbol{E}$ over the surface S. So, if the basis functions project onto N surface expansion functions, N linearly independent surface fields can be constructed from these, and consequently N different solutions of Laplace's equation can occur. The cure to the problem is then to find the N exact Laplace solutions, which can be used to augment the basis set. The augmented basis set gives N zero-values of k^2, and finite values corresponding to uncontaminated Maxwell solutions. This procedure is straightforward, and we shall see how it works in section 5.

4. Array of dielectric slabs

As an initial application of the embedding method we consider the propagation of light through a periodic array of dielectric slabs. Each slab has thickness d, with dielectric constant ϵ, and they are separated by vacuum, with period a in the z-direction. The periodicity means that we need only consider one repeat unit: the vacuum in this unit then constitutes region I, and the single slab is region II.

The easiest way to find the embedding operator for replacing region II is to use (18), from the relationship between the surface-parallel components of $\nabla \times \boldsymbol{E}$ and $\boldsymbol{E}$ in the slab at the trial value of k_0^2. We consider propagation of waves perpendicular to the slab, at this stage, with fields on the left-hand and right-hand surfaces given by

$$E_l \boldsymbol{i} \qquad E_r \boldsymbol{i}. \tag{26}$$

The field inside the slab is then

$$\boldsymbol{E} = [E_+ \exp(\mathrm{i}\kappa z) + E_- \exp(-\mathrm{i}\kappa z)]\boldsymbol{i} \tag{27}$$

with

$$\kappa = \sqrt{\epsilon} k_0. \tag{28}$$

The coefficients are given by

$$\begin{aligned} E_+ &= \frac{E_r \exp(\mathrm{i}\kappa d/2) - E_l \exp(-\mathrm{i}\kappa d/2)}{\exp(\mathrm{i}\kappa d/2) - \exp(-\mathrm{i}\kappa d/2)} \\ E_- &= \frac{E_l \exp(\mathrm{i}\kappa d/2) - E_r \exp(-\mathrm{i}\kappa d/2)}{\exp(\mathrm{i}\kappa d/2) - \exp(-\mathrm{i}\kappa d/2)} \end{aligned} \tag{29}$$

(the origin is in the middle of the slab, though this subsequently drops out). Hence,

$$\begin{aligned} \nabla \times \boldsymbol{E}|_l &= \frac{\kappa[E_r - E_l \cos(\kappa d)]}{\sin(\kappa d)}\boldsymbol{j} \\ \nabla \times \boldsymbol{E}|_r &= -\frac{\kappa[E_l - E_r \cos(\kappa d)]}{\sin(\kappa d)}\boldsymbol{j} \end{aligned} \tag{30}$$

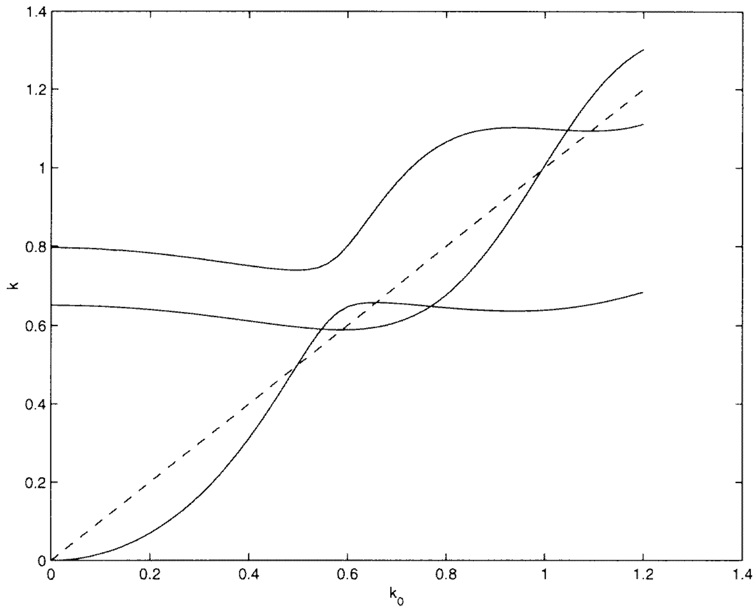

Figure 1. Variation of k with parameter k_0, at $k_z = 0$ with three basis functions. The broken line shows $k = k_0$, and normal modes correspond to where this line intersects a maximum or minimum.

and the embedding operator for constant fields over the surfaces of the slab is

$$\begin{aligned} \boldsymbol{\Sigma}(l,l) = \boldsymbol{\Sigma}(r,r) &= \frac{-\kappa}{\tan(\kappa d)}(\boldsymbol{ii}+\boldsymbol{jj}) \\ \boldsymbol{\Sigma}(l,r) = \boldsymbol{\Sigma}(r,l) &= \frac{-\kappa}{\sin(\kappa d)}(\boldsymbol{ii}+\boldsymbol{jj}). \end{aligned} \tag{31}$$

In region I, between the dielectric slabs, we expand the electric field in plane waves:

$$\boldsymbol{E} = \boldsymbol{i}\sum_n e_n \exp[\mathrm{i}(k_z + 2\pi n/a)z] \tag{32}$$

where k_z is the Bloch wavevector. It is then straightforward to evaluate the matrix elements in (24), with (31) for the embedding potential. In the embedding approach, this expansion is only used for the field in region I; we contrast this with the usual approach in which the plane wave expansion is used for the field in all space [13], minimizing the original variational expression (4).

First we investigate the variation of the eigenvalues k^2 in (23) with k_0^2, the solution parameter in region II. Figure 1 shows the results at $k_z = 0$ with three basis functions, taking the slab thickness $d = 2$, lattice parameter $a = 2\pi$, and slab dielectric constant $\epsilon = 10$. The normal modes of the embedded system correspond to stationary values of k as a function of k_0, where $k = k_0$. At these values Maxwell's equation in region II is solved at the same frequency as in region I. The normal modes can then be found very easily by iterating on k_0.

Tests of the convergence with basis set size are shown in tables 1 and 2. These give the values of k for the four lowest normal modes, at Bloch wavevectors $k_z = 0$ and $k_z = \pi/a$. The top set of results in each table is for the embedding method, and the lower set is evaluated using a plane wave expansion through all space, with the usual variational

Table 1. k-values at $k_z = 0$ for different basis set sizes. Top results are for the embedding method, and lower results for the usual plane wave method.

	k_1	k_2	k_3	k_4
3	0	0.588 56	0.658 06	1.093 68
7	0	0.542 08	0.654 08	1.093 11
11	0	0.540 39	0.654 06	1.093 11
15	0	0.540 34	0.654 06	1.093 11
3	0	0.624 72	0.680 41	—
7	0	0.543 20	0.655 85	1.225 17
11	0	0.541 25	0.654 19	1.098 50
15	0	0.540 56	0.654 12	1.095 87
41	0	0.540 36	0.654 06	1.093 20
Exact	0	0.540 34	0.654 06	1.093 11

Table 2. k-values at $k_z = \pi/a$ for different basis set sizes. Top results are for the embedding method, and lower results for the usual plane wave method.

	k_1	k_2	k_3	k_4
3	0.196 79	0.400 65	0.920 25	0.983 52
7	0.195 44	0.390 72	0.824 65	0.945 17
11	0.195 43	0.390 31	0.821 68	0.945 13
15	0.195 43	0.390 30	0.821 61	0.945 13
3	0.197 58	0.407 01	1.008 26	—
7	0.195 48	0.391 28	0.831 49	1.011 19
11	0.195 45	0.390 54	0.822 08	0.949 44
15	0.195 44	0.390 37	0.821 76	0.947 00
41	0.195 43	0.390 30	0.821 62	0.945 19
Exact	0.195 43	0.390 30	0.821 61	0.945 13

principle (4). We see that the embedding method converges significantly faster than the usual approach. One remarkable aspect of embedding is that we can actually find more bands than basis functions—with only three basis functions we have found the fourth band. This is a consequence of the variation of k with k_0 shown in figure 1, with more extrema at $k = k_0$ than the number of basis functions. Convergence of the k-values is uniform, and in this easy case, with the electric field parallel to the surface of the dielectric, there are no troublesome Laplace solutions. The way that a tiny basis set can yield good results is shown by figure 2, giving the band-structure with three basis functions.

5. Oblique incidence

For a more general case, when Laplace solutions can occur, we now consider light propagating along a layer of vacuum sandwiched between semi-infinite media of dielectric constant less than 1 (figure 3). The light propagates in the x-direction with wavevector k_x, and the electric field lies in the x–z plane—because the electric field has a component normal to the dielectric surface, zero-frequency Laplace solutions can occur.

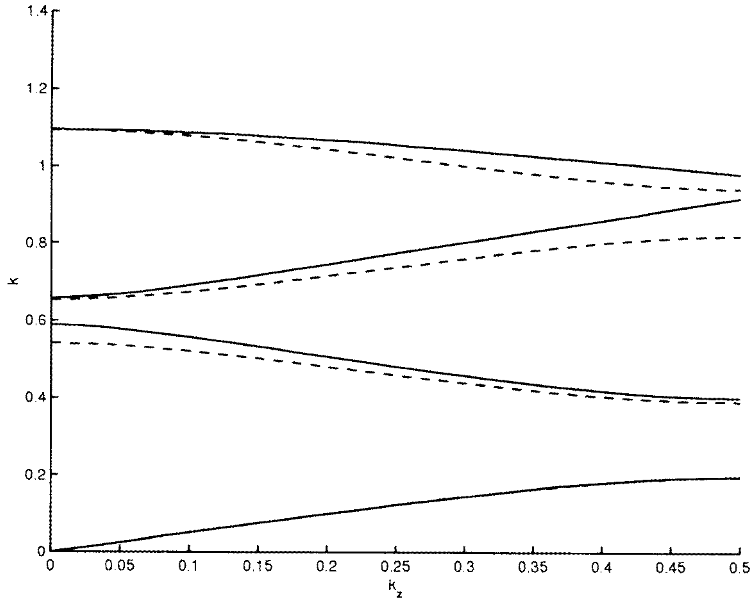

Figure 2. First four bands with three basis functions in the embedding method (full curves), compared with exact results (broken line).

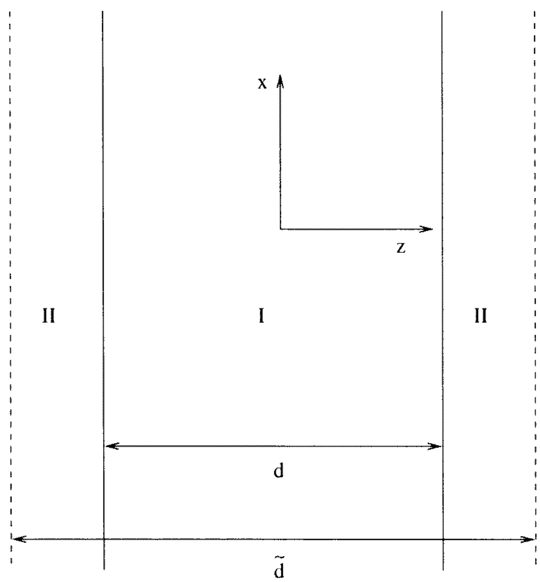

Figure 3. Vacuum sandwiched between dielectric media.

To find the embedding operator to replace the right-hand semi-infinite medium, we first consider an evanescent solution in this region. This has the form

$$\boldsymbol{E} = E_0 \left(\frac{\mathrm{i}\gamma}{\kappa} \boldsymbol{i} - \frac{k_x}{\kappa} \boldsymbol{k} \right) \exp(\mathrm{i} k_x x - \gamma z) \tag{33}$$

with

$$\kappa = \sqrt{\epsilon}k_0 \qquad \text{and } \gamma = \sqrt{k_x^2 - \kappa^2}. \tag{34}$$

So

$$\nabla \times \boldsymbol{E} = E_0 \mathrm{i}\kappa \boldsymbol{j} \exp(\mathrm{i}k_x x - \gamma z) \tag{35}$$

and the embedding operator for evanescent waves is given in this case by

$$\boldsymbol{\Sigma} = \frac{\kappa^2}{\gamma}\boldsymbol{ii}. \tag{36}$$

When $\epsilon k_0^2 > k_x^2$, the solution in the dielectric corresponds to travelling waves, and the embedding operator becomes

$$\boldsymbol{\Sigma} = \frac{\mathrm{i}\kappa^2}{k_z}\boldsymbol{ii} \tag{37}$$

with

$$k_z = \sqrt{\kappa^2 - k_x^2}. \tag{38}$$

$\boldsymbol{\Sigma}$ for the left-hand dielectric is the same as (37).

As our trial function for the electric field in region I, the vacuum between the dielectrics, we take transverse waves:

$$\boldsymbol{E} = \sum_n e_n(-g_n\boldsymbol{i} + k_x\boldsymbol{k}) \exp \mathrm{i}(k_x x + g_n z) \qquad g_n = \frac{2n\pi}{\tilde{d}}. \tag{39}$$

The sum is over integers n, and $\tilde{d}$ is some spacing greater than d (figure 3), so that (39) can produce a range of electric and magnetic fields on the boundaries with the dielectric. It is then straightforward to calculate the matrix elements in (24).

We take a vacuum region of thickness $d = 6$, between media of dielectric constant $\epsilon = 0.5$, and our basis functions are defined by $\tilde{d} = 9$. Table 3 (upper part) shows k-values for the modes with $\epsilon k^2 < k_x^2$, for $k_x = 1$, for different basis set sizes. We see that two of the k-values converge rapidly to the symmetric and antisymmetric waveguide modes which decay exponentially into the media on either side, whereas two other k-values drop to zero. These are the Laplace solutions which correspond to fields varying like $\exp(\mathrm{i}k_x x)$ over the

Table 3. Confined modes in vacuum, thickness $d = 6$, between dielectric media $\epsilon = 0.5$, at $k_x = 1$ for different basis set sizes. Top results are for the electric field embedding method, and lower results from magnetic embedding.

	k_1	k_2	k_3	k_4
3	1.096 42	1.259 59	0.829 65	—
7	1.084 25	1.285 77	0.195 92	0.983 67
11	1.084 07	1.278 89	0.030 04	0.256 40
15	1.084 07	1.278 73	0.004 09	0.048 11
3	1.085 25	1.288 94		
7	1.084 08	1.278 93		
11	1.084 07	1.278 73		
Exact	1.084 07	1.278 73	Laplace	Laplace

Table 4. Confined modes in vacuum, thickness $d = 6$, between dielectric media $\epsilon = 0.5$, at $k_x = 1$, with the augmented basis set and the electric field embedding method. The number of basis functions includes the two exact solutions of Laplace's equation.

	k_1	k_2
5	1.084 22	1.281 26
7	1.084 08	1.278 87
9	1.084 07	1.278 74
11	1.084 07	1.278 73

boundaries of region I. Only these two solutions of Laplace's equation can arise, because there are only two surface degrees of freedom in this case, one for each surface.

Laplace solutions can be avoided in this example by working with the magnetic field rather than the electric field—$\boldsymbol{H}$ in this geometry is parallel to the surfaces. The embedding variational principle for the magnetic field is presented in appendix B, and using the same basis functions as before this gives the modes given in the lower part of table 3. The convergence is even better than with electric field embedding, and uncontaminated by Laplace modes in this geometry.

To suppress the Laplace solutions when the field has a surface-normal component, we augment the basis set with exact solutions of Laplace's equation. In this case, when the field has the variation $\exp(\mathrm{i}k_x x)$ over the boundary of region I, we add onto (39) electric fields corresponding to the electrostatic potentials:

$$\phi_\pm = \exp(\mathrm{i}k_x x \pm k_x z). \tag{40}$$

The electric field variational principle then gives two modes with exactly zero k-value, and the two confined solutions of Maxwell's equations converge very satisfactorily (table 4). This is the solution to the problem caused by the Laplace solutions—by augmenting the basis set, these modes drop to zero out of harm's way. It should in general be very easy to find suitable augmenting solutions: they are the fields produced by surface charge densities on the boundaries of region I, with the different possible functional forms given by projecting the basis functions onto the boundaries. The matrix elements involving Laplace solutions can be reduced to surface integrals, via the divergence theorem. Moreover, these solutions only depend on the geometry of region I, and are independent of the system in region II onto which it is embedded.

The embedding method makes it very easy to find continuum states, as well as the discrete waveguide modes. In the continuum, rather than work with individual eigenfunctions of (1)

$$\nabla \times \nabla \times \boldsymbol{E}_i = \epsilon(\boldsymbol{r}) k_i^2 \boldsymbol{E}_i \tag{41}$$

we work with the spectral density

$$n(\boldsymbol{r}, k^2) = \sum_i \epsilon(\boldsymbol{r}) \boldsymbol{E}_i(\boldsymbol{r}) \cdot \boldsymbol{E}_i(\boldsymbol{r}) \delta(k^2 - k_i^2). \tag{42}$$

This can be written in terms of the tensor Green function (13), which in a spectral representation [24] is given by

$$\boldsymbol{\Gamma}(\boldsymbol{r}, \boldsymbol{r}'; k^2) = \sum_i \frac{\boldsymbol{E}_i(\boldsymbol{r}) \boldsymbol{E}_i(\boldsymbol{r}')}{k_i^2 - k^2}. \tag{43}$$

Here $\boldsymbol{E}_i$ is normalized including $\epsilon(\boldsymbol{r})$ as a weighting function, as in (4):

$$\int \mathrm{d}\boldsymbol{r}\, \epsilon(\boldsymbol{r}) \boldsymbol{E}_i(\boldsymbol{r}) \cdot \boldsymbol{E}_i(\boldsymbol{r}) = 1. \tag{44}$$

So we see that

$$n(\boldsymbol{r}, k^2) = \frac{1}{\pi} \epsilon(\boldsymbol{r}) \mathrm{Im}\, \boldsymbol{\Gamma}(\boldsymbol{r}, \boldsymbol{r}; k^2 + \mathrm{i}\delta) \tag{45}$$

where δ is infinitesimal. The Green function for $\boldsymbol{r}$, $\boldsymbol{r}'$ in region I can be expanded in the basis set used in (22):

$$\boldsymbol{\Gamma}(\boldsymbol{r}, \boldsymbol{r}'; k^2) = \sum_{ij} \Gamma_{ij}(k^2) \boldsymbol{F}_i(\boldsymbol{r}) \boldsymbol{F}_j(\boldsymbol{r}') \tag{46}$$

where Γ_{ij} satisfies the inhomogeneous equation

$$\sum_k (A_{ik} - k^2 B_{ik}) \Gamma_{kj} = \delta_{ij}. \tag{47}$$

Matrices A and B are given by (24), but without the $\partial/\partial k_0^2$ terms, as the embedding operator is evaluated at the same value of k^2 as the Green function. Then the spectral density, which we shall evaluate integrated through region I, is given by

$$n_{\mathrm{I}}(k^2) = \frac{1}{\pi} \sum_{ij} \mathrm{Im}\, \Gamma_{ij}(k^2 + \mathrm{i}\delta) \int_{\mathrm{I}} \mathrm{d}\boldsymbol{r}\, \epsilon \boldsymbol{F}_i \cdot \boldsymbol{F}_j. \tag{48}$$

Figure 4 shows the spectral density in region I for this problem of the vacuum sandwiched between the dielectric slabs. The augmented basis set is used, with 11 basis functions including the two Laplace solutions. The imaginary part of k^2 has been set to 0.005, to broaden the discrete states. We see clearly how the embedding method can find continuum states and discrete states in a simple way, on the same footing.

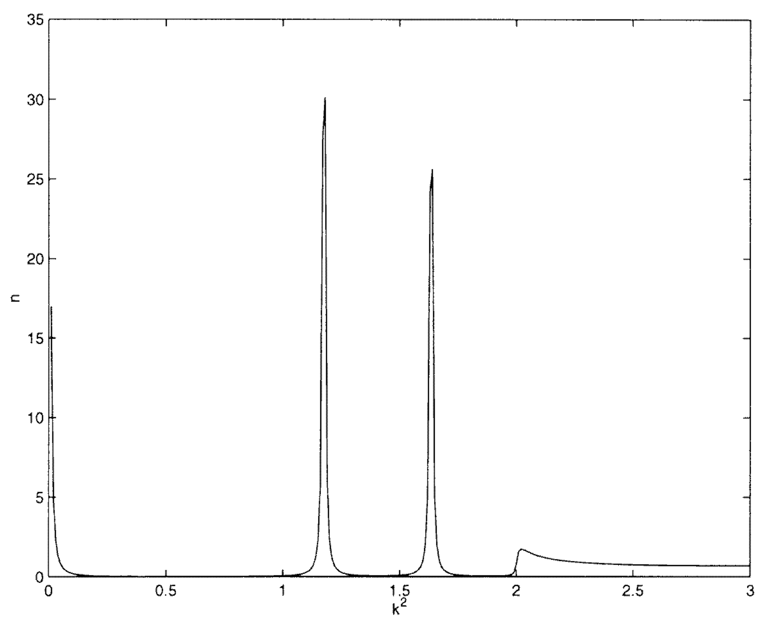

Figure 4. Spectral density in vacuum, thickness $d = 6$, between dielectric media $\epsilon = 0.5$, at $k_x = 1$, with 11 basis functions in the augmented basis set. k^2 has an imaginary part of 0.005.

6. Confinement by conducting walls

The reflection of electromagnetic waves at the surface of a good conductor can be treated quite simply, using the embedding method to replace the conducting medium by an embedding operator at its boundary. Loss processes in the conductor lead to a complex embedding operator, which broadens discrete states.

We find the embedding operator again from (18), using the known solutions of Maxwell's equations near the surface of a good conductor [35]. Taking the z-axis directed into the conductor, the magnetic and electric fields are given by

$$\begin{aligned} \boldsymbol{H} &= \boldsymbol{j} H_0 \exp[z(\mathrm{i}-1)/\delta] \\ \boldsymbol{E} &= \boldsymbol{i}\sqrt{\frac{\omega}{8\pi\sigma}}(1-\mathrm{i})H_0 \exp[z(\mathrm{i}-1)/\delta] \end{aligned} \tag{49}$$

where ω is the frequency, σ is the conductivity, and the skin depth is given by $\delta = c/\sqrt{2\pi\omega\sigma}$. The electric field and its curl at the surface are then given by

$$\begin{aligned} \boldsymbol{E} &= \boldsymbol{i}\sqrt{\frac{\omega}{8\pi\sigma}}(1-\mathrm{i})H_0 \\ \nabla \times \boldsymbol{E} &= \boldsymbol{j}\frac{\mathrm{i}\omega}{c}H_0 \end{aligned} \tag{50}$$

hence the embedding tensor is

$$\boldsymbol{\Sigma}(\boldsymbol{r}_S, \boldsymbol{r}'_S) = (\mathrm{i}-1)\frac{\sqrt{2\pi\omega\sigma}}{c}[\boldsymbol{ii} + \boldsymbol{jj}]\delta(\boldsymbol{r}_S - \boldsymbol{r}'_S). \tag{51}$$

It is a local operator, because of the short skin depth in a good conductor, and this means that we can use (51) at a surface of arbitrary shape. The imaginary part of $\boldsymbol{\Sigma}$ is due to loss processes in the conductor, which are fully taken account in the formalism.

As a simple application, we consider electromagnetic waves confined inside a cubic metal box, side d. The interior of the box constitutes region I, and we replace the surrounding metal by the embedding potential (51) on the boundary. We then calculate the Green function using a basis of transverse travelling waves, with wavevectors $\frac{2\pi}{\tilde{d}}(h, k, l)$; we take $\tilde{d}$, the fundamental wavelength, to be a little larger than $2d$ in this case. In units with $c = 1$, a box-side $d = 6$, $\tilde{d} = 13$, and the conductivity $\sigma = 1000$, we obtain the results shown in figure 5 for the spectral density integrated through region I. Both the position and the width of the peaks converge well with basis set size—it is interesting to see how the second peak sharpens up in going from 57 wavevectors to 87, whereas the third peak is given well with the smaller basis set. In this case no problems associated with Laplace solutions arise, because the metal boundary condition eliminates them. Presumably a much smaller basis set could be used if it was specially constructed to match the box geometry, but we have chosen plane waves as these could be used easily with more complicated boundaries.

The problem of electromagnetic waves confined by a conductor is analogous to the confinement of electrons by a very deep potential well, for which the embedding method also provides a highly efficient method of solution [22]. As in the Schrödinger equation case, where extremely deep wells corresponding to almost perfect confinement can be treated, we expect that very high conductivities can be handled in this case. Projection operator techniques with a plane wave basis set have recently been developed to handle perfect conductors [36], and it will be interesting to compare the two approaches.

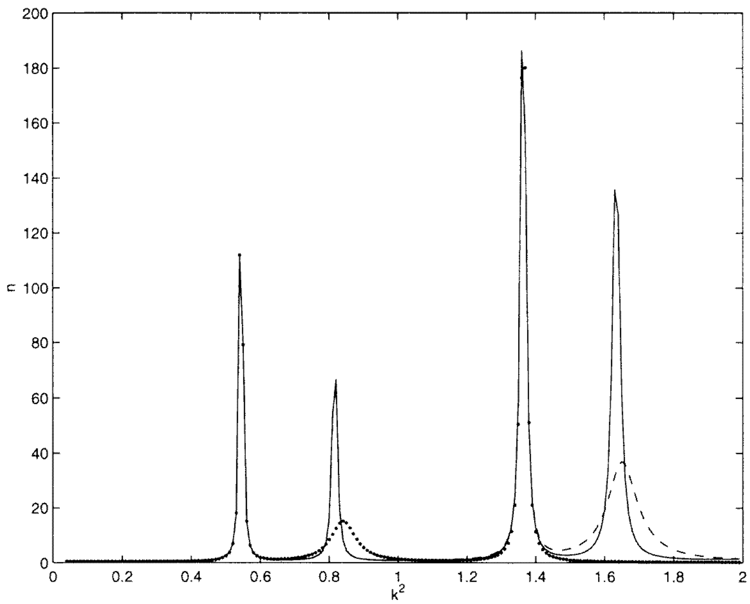

Figure 5. Spectral density in the interior of a metal box, sides $d = 6$, conductivity $\sigma = 1000$ (in units with $c = 1$). Transverse plane waves with $\tilde{d} = 13$ are used as basis functions; the dotted curve indicates 57 wavevectors, the broken curve indicates 87, and the full curve indicates 111 wavevectors in the basis set.

Appendix A

In this appendix we consider variations in (20). Using the fact that the embedding operator is symmetric, the change in k^2 due to a small change in the trial field $\delta\mathcal{E}$ is given by

$$\delta k^2 = 2\frac{\int_{\mathrm{I}} \mathrm{d}\boldsymbol{r}\,(\nabla\times\delta\mathcal{E})\cdot(\nabla\times\mathcal{E}) - \int_S \mathrm{d}r_S \int_S \mathrm{d}r'_S\,(\boldsymbol{n}\times\delta\mathcal{E})\cdot(\boldsymbol{\Sigma} - k_0^2\frac{\partial\boldsymbol{\Sigma}}{\partial k_0^2})\cdot(\boldsymbol{n}\times\mathcal{E})}{\int_{\mathrm{I}} \mathrm{d}\boldsymbol{r}\,\epsilon\mathcal{E}\cdot\mathcal{E} + \int_S \mathrm{d}r_S \int_S \mathrm{d}r'_S\,(\boldsymbol{n}\times\mathcal{E})\cdot\frac{\partial\boldsymbol{\Sigma}}{\partial k_0^2}\cdot(\boldsymbol{n}\times\mathcal{E})}$$
$$-2k^2\frac{\int_{\mathrm{I}} \mathrm{d}\boldsymbol{r}\,\epsilon\delta\mathcal{E}\cdot\mathcal{E} + \int_S \mathrm{d}r_S \int_S \mathrm{d}r'_S\,(\boldsymbol{n}\times\delta\mathcal{E})\cdot\frac{\partial\boldsymbol{\Sigma}}{\partial k_0^2}\cdot(\boldsymbol{n}\times\mathcal{E})}{\int_{\mathrm{I}} \mathrm{d}\boldsymbol{r}\epsilon\mathcal{E}\cdot\mathcal{E} + \int_S \mathrm{d}r_S \int_S \mathrm{d}r'_S\,(\boldsymbol{n}\times\mathcal{E})\cdot\frac{\partial\boldsymbol{\Sigma}}{\partial k_0^2}\cdot(\boldsymbol{n}\times\mathcal{E})}. \tag{A.1}$$

Using the vector identity (3) and the divergence theorem, this becomes

$$\delta k^2 = 2\Bigg[\bigg(\int_{\mathrm{I}} \mathrm{d}\boldsymbol{r}\,\delta\mathcal{E}\cdot(\nabla\times\nabla\times\mathcal{E}) - k^2\int_{\mathrm{I}} \mathrm{d}\boldsymbol{r}\,\epsilon\delta\mathcal{E}\cdot\mathcal{E}\bigg) + \bigg(\int_S \mathrm{d}r_S\,(\boldsymbol{n}\times\delta\mathcal{E})\cdot(\nabla\times\mathcal{E})$$
$$- \int_S \mathrm{d}r_S \int_S \mathrm{d}r'_S(\boldsymbol{n}\times\delta\mathcal{E})\cdot\left\{\boldsymbol{\Sigma} + (k^2 - k_0^2)\frac{\partial\boldsymbol{\Sigma}}{\partial k_0^2}\right\}\cdot(\boldsymbol{n}\times\mathcal{E})\bigg)\Bigg]$$
$$\Bigg/\Bigg[\int_{\mathrm{I}} \mathrm{d}\boldsymbol{r}\,\epsilon\mathcal{E}\cdot\mathcal{E} + \int_S \mathrm{d}r_S \int_S \mathrm{d}r'_S\,(\boldsymbol{n}\times\mathcal{E})\cdot\frac{\partial\boldsymbol{\Sigma}}{\partial k_0^2}\cdot(\boldsymbol{n}\times\mathcal{E})\Bigg]. \tag{A.2}$$

This is zero for arbitrary changes $\delta\mathcal{E}$ within region I when $\mathcal{E}$ satisfies

$$\nabla\times\nabla\times\mathcal{E} = \epsilon(\boldsymbol{r})k^2\mathcal{E} \tag{A.3}$$

and for arbitrary $\delta\mathcal{E}$ on the boundary when the surface-parallel components satisfy

$$\nabla\times\mathcal{E} = \int_S \mathrm{d}r'_S\,\left\{\boldsymbol{\Sigma}|_{k_0^2} + (k^2 - k_0^2)\frac{\partial\boldsymbol{\Sigma}}{\partial k_0^2}\right\}\cdot(\boldsymbol{n}\times\mathcal{E}). \tag{A.4}$$

The first condition is of course the wave equation we are trying to satisfy, and the second condition means that the surface-parallel components of $\nabla \times \boldsymbol{E}$, as well as $\boldsymbol{E}$, match on either side of the boundary. What is remarkable about the second condition is that the derivative $\partial \boldsymbol{\Sigma}/\partial k_0^2$, which started off life in the normalization of the field in region II, corrects the embedding operator so that to first order in $(k^2 - k_0^2)$ it is evaluated at the correct value of k^2.

Appendix B

If the dielectric constant ϵ is constant, the wave equation for the magnetic field has the same form as (1):

$$\nabla \times \nabla \times \boldsymbol{H} = \epsilon \frac{\omega^2}{c^2} \boldsymbol{H} \tag{B.1}$$

and the boundary conditions across a boundary between dielectrics are that the surface-parallel components of $\boldsymbol{H}$ and $\frac{1}{\epsilon}\nabla \times \boldsymbol{H}$ are continuous. For a magnetic variational principle analogous to (20), we define an embedding operator replacing region II by

$$\frac{1}{\epsilon_{\mathrm{II}}} \nabla \times \boldsymbol{H}|_{\boldsymbol{r}_S} = \int_S \mathrm{d}r'_S \, \boldsymbol{\Sigma}^m(\boldsymbol{r}_S, \boldsymbol{r}'_S) \cdot (\boldsymbol{n} \times \mathcal{H}) \tag{B.2}$$

—again only surface-parallel components—where ϵ_{II} is the dielectric constant in region II and $\mathcal{H}$ is the trial value of the magnetic field on the surface S.

We consider now the expression:

$$k^2 = \frac{\frac{1}{\epsilon_{\mathrm{I}}} \int_{\mathrm{I}} \mathrm{d}\boldsymbol{r} \, (\nabla \times \mathcal{H}) \cdot (\nabla \times \mathcal{H}) - \int_S \mathrm{d}r_S \int_S \mathrm{d}r'_S \, (\boldsymbol{n} \times \mathcal{H}) \cdot (\boldsymbol{\Sigma}^m - k_0^2 \frac{\partial \boldsymbol{\Sigma}^m}{\partial k_0^2}) \cdot (\boldsymbol{n} \times \mathcal{H})}{\int_{\mathrm{I}} \mathrm{d}\boldsymbol{r} \, \mathcal{H} \cdot \mathcal{H} + \int_S \mathrm{d}r_S \int_S \mathrm{d}r'_S \, (\boldsymbol{n} \times \mathcal{H}) \cdot \frac{\partial \boldsymbol{\Sigma}^m}{\partial k_0^2} \cdot (\boldsymbol{n} \times \mathcal{H})}. \tag{B.3}$$

Using the same arguments as in appendix A, this is stationary when $\mathcal{H}$ satisfies (B.1) in region I, and on the boundary with II the surface-parallel components satisfy:

$$\frac{1}{\epsilon_{\mathrm{I}}} \nabla \times \mathcal{H} = \int_S \mathrm{d}r'_S \left\{ \boldsymbol{\Sigma}^m|_{k_0^2} + (k^2 - k_0^2) \frac{\partial \boldsymbol{\Sigma}^m}{\partial k_0^2} \right\} \cdot (\boldsymbol{n} \times \mathcal{H}). \tag{B.4}$$

This means that the surface-parallel components of $\frac{1}{\epsilon}\nabla \times \boldsymbol{H}$ and $\boldsymbol{H}$ match on either side of the boundary, as we require.

The restriction to constant ϵ within each region in (B.1) and (B.3) does not apply to the electric field expression (20), because of the form of Maxwell's equations.

References

[1] Joannopoulos J D, Villeneuve P R and Fan S 1997 *Nature* **386** 143
[2] Leung K M and Liu Y F 1990 *Phys. Rev. Lett.* **65** 2646
[3] Zhang Z and Satpathy S 1990 *Phys. Rev. Lett.* **65** 2650
[4] Ho K M, Chan C T and Soukalis C M 1990 *Phys. Rev. Lett.* **65** 3152
[5] Haus J W 1994 *J. Mod. Opt.* **41** 195
[6] Robertson W M, Arjavalingam G, Meade R D, Brommer K D, Rappe A M and Joannopoulos J D 1992 *Phys. Rev. Lett.* **68** 2023
[7] Yablanovitch E 1993 *J. Phys.: Condens. Matter* **5** 2443
[8] Cheng C C and Scherer A 1995 *J. Vac. Sci. Technol.* B **13** 2696
[9] Grüning U, Lehmann V, Ottow S and Busch K 1996 *Appl. Phys. Lett.* **68** 747
[10] Mekis A, Chen J C, Kurland I, Fan S, Villeneuve P R and Joannopoulos J D 1996 *Phys. Rev. Lett.* **77** 3787

[11] Stratton J A 1941 *Electromagnetic Theory* (New York: McGraw-Hill)
[12] Sözüer H S, Haus J W and Inguva R 1992 *Phys. Rev.* B **45** 13 962
[13] Villeneuve P R and Piché M 1994 *J. Mod. Opt.* **41** 241
[14] Pendry J B and MacKinnon A 1992 *Phys. Rev. Lett.* **69** 2772
[15] Pendry J B 1994 *J. Mod. Opt.* **41** 209
[16] Tsai Y-C, Shung K W-K and Pendry J B 1998 *J. Phys.: Condens. Matter* **10** 753
[17] Modinos A 1987 *Physica* **141A** 575
[18] Wang X, Zhang X-G, Yu Q and Harmon B N 1993 *Phys. Rev.* B **47** 4161
[19] Ohtaka K, Ueta T and Amemiya K 1998 *Phys. Rev.* B **57** 2550
[20] Inglesfield J E 1981 *J. Phys. C: Solid State Phys.* **14** 3795
[21] Crampin S, van Hoof J B A N, Nekovee M and Inglesfield J E 1992 *J. Phys.: Condens. Matter* **4** 1475
[22] Crampin S, Nekovee M and Inglesfield J E 1995 *Phys. Rev.* B **51** 7318
[23] Thijssen J M and Inglesfield J E 1994 *Europhys. Lett.* **27** 65
[24] Cairo L and Kahan T 1965 *Variational Techniques in Electromagnetism* (New York: Gordon and Breach)
[25] English W J 1971 *IEEE* **MTT-19** 9
[26] Konrad A 1976 *IEEE* **MTT-24** 553
[27] Jeng S-K and Chen C-H 1984 *IEEE* **AP-32** 902
[28] Wu R-B and Chen C-H 1985 *IEEE* **MTT-33** 477
[29] Chung S-J and Chen C-H 1988 *IEEE* **MTT-36** 473
[30] Pearson L W, Peterson A F, Bahrmasel L J and Whitaker R A 1992 *IEEE* **AP-40** 714
[31] McDonald B H and Wexler A 1972 *IEEE* **MTT-20** 841
[32] Zienkiewicz O C, Kelly D W and Bettess P 1977 *Int. J. Numer. Meth. Eng.* **11** 355
[33] Senior T B A 1981 *IEEE* **AP-29** 826
[34] Senior T B A and Volakis J L 1995 *Approximate Boundary Conditions in Electromagnetics* (London: The Institution of Electrical Engineers)
[35] Jackson J D 1962 *Classical Electrodynamics* (New York: Wiley)
[36] Suzuki T and Yu P K-L 1998 *Phys. Rev.* B **57** 2229